

Nonlinear and Negative Effective Diffusivity of Interlayer Excitons in Moiré-Free Heterobilayers

Edith Wietek¹, Matthias Florian², Jonas Göser³, Takashi Taniguchi⁴, Kenji Watanabe⁵, Alexander Högele⁶, Mikhail M. Glazov⁷, Alexander Steinhoff^{8,9} and Alexey Chernikov^{1,*}

¹Institute of Applied Physics and Würzburg-Dresden Cluster of Excellence ct.qmat, Technische Universität Dresden, 01062 Dresden, Germany

²Department of Electrical Engineering and Computer Science, University of Michigan, Ann Arbor, Michigan 48109, USA

³Fakultät für Physik, Munich Quantum Center, and Center for NanoScience (CeNS), Ludwig-Maximilians-Universität München, 80539 München, Germany

⁴Research Center for Materials Nanoarchitectonics, National Institute for Materials Science, I-1 Namiki, Tsukuba 305-0044, Japan

⁵Research Center for Electronic and Optical Materials, National Institute for Materials Science, I-1 Namiki, Tsukuba 305-0044, Japan

⁶Munich Center for Quantum Science and Technology (MCQST), 80799 München, Germany
⁷Ioffe Institute, 194021 Saint Petersburg, Russian Federation

⁸Institut für Theoretische Physik, Universität Bremen, 28334 Bremen, Germany

⁹Bremen Center for Computational Materials Science, Universität Bremen, 28334 Bremen, Germany



(Received 3 August 2023; accepted 10 November 2023; published 4 January 2024)

Interlayer exciton diffusion is studied in atomically reconstructed MoSe₂/WSe₂ heterobilayers with suppressed disorder. Local atomic registry is confirmed by characteristic optical absorption, circularly polarized photoluminescence, and g-factor measurements. Using transient microscopy we observe propagation properties of interlayer excitons that are independent from trapping at moiré- or disorder-induced local potentials. Confirmed by characteristic temperature dependence for free particles, linear diffusion coefficients of interlayer excitons at liquid helium temperature and low excitation densities are almost 1000 times higher than in previous observations. We further show that exciton-exciton repulsion and annihilation contribute nearly equally to nonlinear propagation by disentangling the two processes in the experiment and simulations. Finally, we demonstrate effective shrinking of the light emission area over time across several hundreds of picoseconds at the transition from exciton- to the plasma-dominated regimes. Supported by microscopic calculations for band gap renormalization to identify the Mott threshold, this indicates transient crossing between rapidly expanding, short-lived electron-hole plasma and slower, long-lived exciton populations.

DOI: 10.1103/PhysRevLett.132.016202

Within the rich family of van der Waals heterostructures [1,2], artificially stacked bilayers of semiconducting transition metal dichalcogenides emerged as a highly interesting platform for condensed matter research [3,4]. They offer novel pathways to design electronic states by tuning local atomic registries through angular and lattice mismatch [5–11], revealing a plethora of many-body phenomena [12–14]. Importantly, electron-hole excitations in these systems are governed by strong Coulomb interaction, forming tightly bound excitons [3,15]. They often involve spatially separated electron and hole constituents, conceptually similar to the excitons in coupled quantum wells [16,17]. These interlayer excitons (IXs) can be long-lived [18], manipulated and guided by external fields [19], exhibit long valley-polarization lifetimes [20], and demonstrate correlated phenomena [14,21]. They

emerged as the main carriers of energy and quantum information in van der Waals heterostructures. Naturally, the question of how the excitons propagate attracted an increasing amount of attention, bridging the realms of optics and transport [20,22–27] with promising pathways toward excitonic devices [19,28].

Despite recent progress, however, it remains very challenging to disentangle intrinsic and extrinsic phenomena associated with van der Waals heterostructures that determine exciton transport. Primarily, these include trapping due to disorder from strain and dielectric effects [29] or within the moiré-induced potentials [5–11]. Both induce localization of excitons, evidenced by vanishing diffusion coefficients, observed at low temperatures [26,27]. Exciton-exciton interactions further lead to strongly nonlinear effects, typically considered to stem from

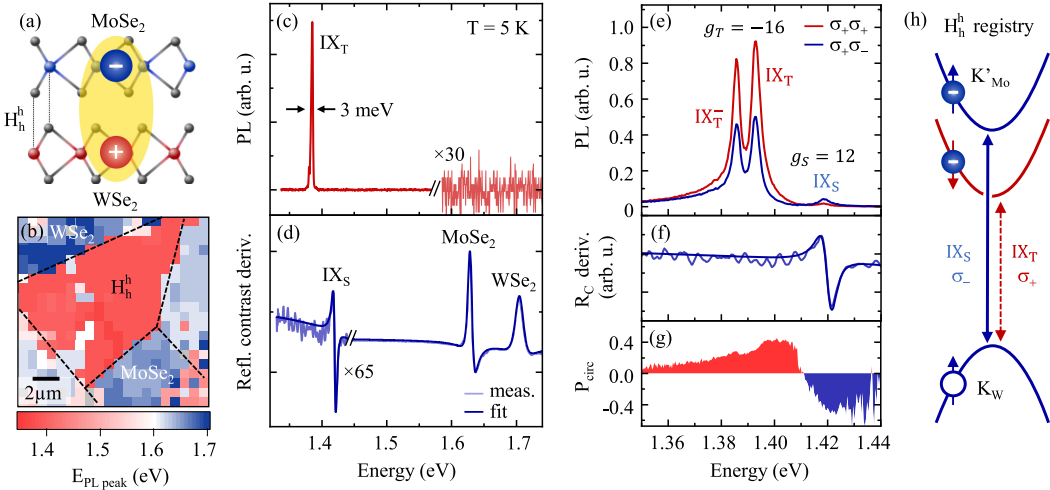


FIG. 1. (a) Schematic illustration of an interlayer exciton in a H_h^h reconstructed MoSe₂/WSe₂ heterobilayer. (b) PL peak energy map at $T = 5$ K. (c) Representative PL spectrum under low-density pumping. (d) Reflectance contrast derivative with fit from transfer matrix analysis. (e) Circularly polarized PL after σ_+ polarized, pulsed excitation with g factors from magneto-optical measurements. (f) Reflectance contrast derivative R_C and (g) degree of circular polarization $P_{\text{circ}} = (I_+ - I_-)/(I_+ + I_-)$. (h) Optical selection rules for H_h^h -stacked MoSe₂/WSe₂ heterobilayer (adapted from Ref. [39]).

dipolar repulsion in analogy to coupled quantum wells [17,24,27,28,30,31]. In contrast, exciton-exciton annihilation often determines effective diffusion in the monolayer constituents [32,33]. Finally, the Mott transition from excitons to plasma already occurs at excitation densities of a few 10^{12} cm^{-2} [34], leading to observations of rapid effective diffusion [27,35]. To understand exciton propagation in van der Waals heterobilayers, the following questions thus need to be resolved: What are the pristine properties of propagating interlayer excitons in the *absence* of disorder and moiré potentials? Which nonlinear effects are important and how can they be distinguished? Is there any *qualitative* impact of excitons and plasma on the propagation dynamics at the Mott transition?

Here, we address these questions by focusing on interlayer excitons in a prototypical heterobilayer system, MoSe₂/WSe₂, schematically illustrated in Fig. 1. Taking advantage of the recently demonstrated conditions for atomic reconstruction [36–38], we realize the scenario of sufficiently large, moiré-free domains with fixed interlayer registry. The encapsulation in high-quality hexagonal boron nitride (h -BN) suppresses extrinsic sources of disorder. Employing time-resolved optical microscopy, we find that interlayer excitons are highly mobile even at low densities and cryogenic temperatures. The measured diffusion coefficients are almost 1000 times higher than previously reported at comparable conditions in moiré systems [26,27]. The absence of trapping is strongly supported by a characteristic temperature dependence for free propagation. Further, we disentangle two main sources of nonlinear diffusion, demonstrating nearly equal contributions from exciton-exciton repulsion and annihilation. Finally, we show that propagation dynamics of optically

induced excitations undergo a substantial change above the Mott transition. Most strikingly, it leads to the appearance of *negative* effective diffusion, indicating transient crossing between plasma- and exciton-dominated regimes.

The h -BN-encapsulated MoSe₂/WSe₂ heterostructures were fabricated by mechanical exfoliation and dry viscoelastic transfer [40]. Matching angular alignment was confirmed by second-harmonic generation measurements, indicating H -type stacking; see Supplemental Material [41]. The samples were placed in a liquid-helium microscopy-cryostat and closed-cycle magnetocryostat for transient diffusion and g -factor measurements, respectively. For photoluminescence (PL) studies, we employed both continuous-wave excitation (2.33 eV photon energy) and Ti: sapphire laser (80 MHz repetition rate, 140 fs pulses) tuned to the photon energy of the MoSe₂ A exciton of 1.63 eV. Reflectance measurements were performed using a tungsten halogen lamp. The signals were resolved spectrally and spatially by a grating and a mirror, respectively. They were detected either by a charged-coupled device or by a streak camera. Detailed description of the setup is outlined in Refs. [32,127] and the Supplemental Material [41].

As illustrated in Fig. 1(b), the PL of the heterostructure region appears at photon energies around 1.4 eV at $T = 5$ K, as expected for IXs in MoSe₂/WSe₂ [18]. A typical spectrum at low-density, continuous-wave excitation is dominated by a single peak with 3 meV linewidth [Fig. 1(c)]. No emission from the intralayer excitons is detected. The IX PL is accompanied by a sharp resonance in the reflectance contrast derivative spectrum, presented in Fig. 1(d). Its oscillator strength is determined to be about 2% of the intralayer excitons, consistent with Refs. [39,122]. This implies good interlayer contact for

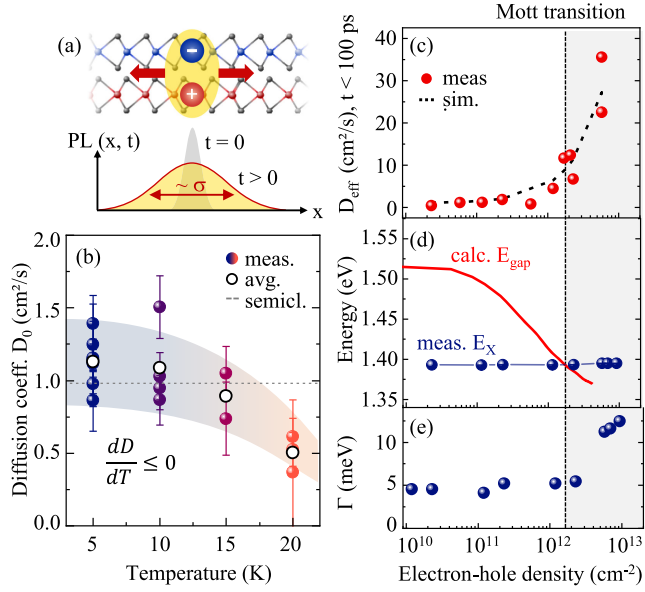


FIG. 2. (a) Schematic illustration of transient microscopy. (b) Temperature-dependent, linear diffusion coefficient D_0 at injection density of $1.2 \times 10^{11} \text{ cm}^{-2}$ electron-hole pairs per pulse ($0.5 \mu\text{J cm}^{-2}$). (c) Effective diffusion coefficients extracted during the first 100 ps. (d) Calculated free particle band gap, renormalized due to the presence of free charge carriers, and measured exciton peak energy. (e) Line shape broadening at the Mott transition.

sufficient electron-hole wave function overlap and the presence of atomic reconstruction. Most importantly, the reflectance contrast spectrum above 1.5 eV is a superposition of the individual MoSe₂ and WSe₂ monolayer spectra, slightly shifted and broadened. No resonance splitting and redistribution of the oscillator strengths are observed, demonstrating the absence of moiré potentials [8]. Circularly polarized PL indicates emission from spin singlets IX_S and spin triplets IX_T with high and low oscillator strengths, respectively, presented in Figs. 1(e)–1(g). They correspond to the $K_{\text{W}}-K'_{\text{Mo}}$ electronic transitions, consistent with the optical selection rules of the H_h^h registry, illustrated in Fig. 1(h) [39]. The lowest energy peak stems from IX_T⁻ trions [23,123–125] due to weak nonintentional doping below 10^{11} cm^{-2} , as observed in gate-dependent measurements (see Supplemental Material [41]). Finally, both the absolute peak energies and the g factors obtained from magneto-PL of $g_S = 12$ and $g_T = -16$ strongly support the $K-K'$ transitions and H_h^h registry assignment [38,126].

To demonstrate that IXs are free to move in the absence of moiré localization and disorder across a spatially extended, reconstructed domain we perform spatially and time-resolved exciton diffusion experiments, Fig. 2(a), at low pump power and as a function of temperature. Measured linear diffusion coefficients D_0 , extracted within the IX lifetime below 1 ns (see Supplemental Material [41]),

are presented in Fig. 2(b). Notably, the average value of $1.1 \pm 0.2 \text{ cm}^2/\text{s}$ at $T = 5 \text{ K}$ is about 1000 times higher than previously found for moiré potentials at low densities [26,27]. The diffusion matches the semiclassical (semicl. in Fig. 2) expectation of $D_0 = 0.98 \text{ cm}^2/\text{s}$ using the scattering time obtained from the spectral broadening (see Supplemental Material [41]) and it decreases with temperature. It corresponds to effective mobility of more than $2000 \text{ cm}^2/(\text{Vs})$ and diffusion length on the order of $0.5 \mu\text{m}$. The physics of IX propagation in the heterostructure thus closely resemble those of WSe₂ monolayers [127], with the 5 K diffusion being determined by the exciton-phonon interaction. Rapid diffusion of free IXs further rationalizes comparatively short lifetimes due to associated increase of the nonradiative capture probability [128].

Nonlinear propagation is presented in Fig. 2(c) as a function of optically injected electron-hole pair density n_{eh} . The effective diffusion coefficient, evaluated during the first 100 ps after the excitation, increases above $30 \text{ cm}^2/\text{s}$ at $n_{\text{eh}} = 6 \times 10^{12} \text{ cm}^{-2}$. These densities cover the Mott transition from excitons to electron-hole plasma, typically found in MoSe₂/WSe₂ heterostructures in this range [34]. Using the theoretical approach from Refs. [34,129], we determine the Mott threshold by calculating the renormalization of the quasiparticle band gap as a function of electron-hole density (see Supplemental Material [41]) for the studied H_h^h registry. The assumptions of the model based on free carriers should be applicable close to the Mott transition. The absolute energy of the band gap is fixed for the lowest densities to the sum of the exciton peak energy and the exciton binding energy. The latter was set to 130 meV in heterobilayers according to both calculated value and literature [15]. The Mott threshold is estimated from the crossing of the calculated band gap and measured exciton peak energies, see Fig. 2(d). The obtained value of $2 \times 10^{12} \text{ cm}^{-2}$ is consistent with literature [34] and further supported by the onset of spectral broadening [Fig. 2(e)].

The origin of the nonlinear increase of the effective diffusion coefficient is commonly attributed to exciton-exciton annihilation (EEA) in monolayers [32,33] and exciton-exciton repulsion in heterostructures [24,27] and coupled quantum wells [130]. These two processes enter the diffusion equation as the last two terms in

$$\frac{\partial n}{\partial t} = D_0 \Delta n - \frac{n}{\tau} - R_A n^2 + \frac{U_0 D_0}{k_B T} \nabla \cdot (n \nabla n), \quad (1)$$

where D_0 and τ are the linear diffusion coefficient and exciton lifetime at low densities, respectively, R_A is the annihilation rate coefficient, U_0 is the interaction constant ($U_0 n$ corresponds to the blueshift of the exciton peak), and k_B is the Boltzmann constant. We solve Eq. (1) numerically by using the initial shape of the excitation spot as a boundary condition, fixing D_0 and τ to the measured

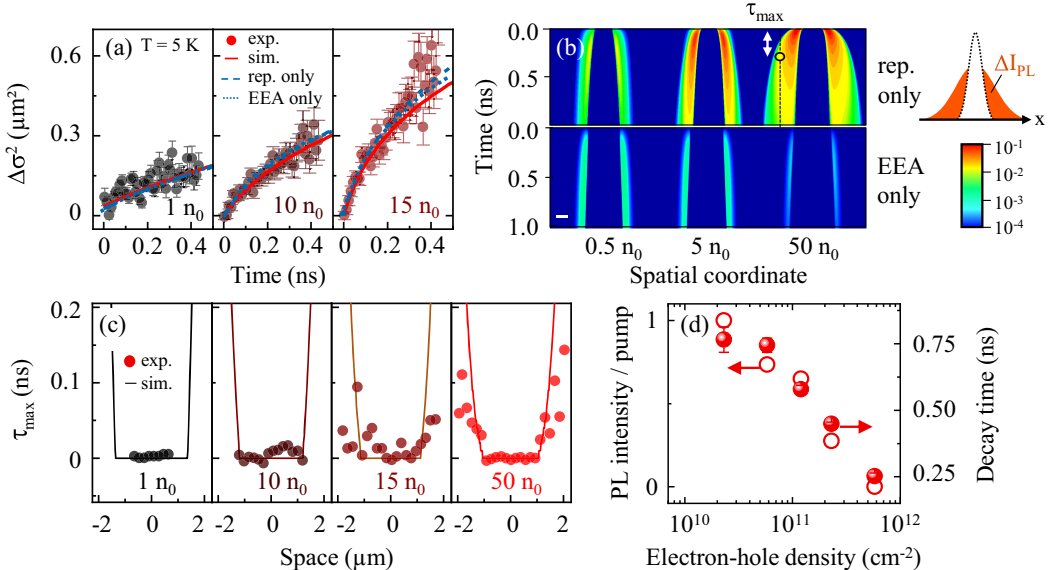


FIG. 3. (a) Mean-squared displacement of IX for selected densities in units of $n_0 = 1.2 \times 10^{11} \text{ cm}^{-2}$. Lines represent simulation results using Eq. (1) due to annihilation only (dotted), repulsion only (dashed), and their combination (solid). (b) Simulated relative increase of $\Delta I_{\text{PL}} = [I_{\text{PL}}(t) - I_{\text{PL}}(0)]/I_{\text{PL,max}}$; scale bar is $1 \mu\text{m}$. (c) Spatially dependent time τ_{max} for the PL to reach its maximum, extracted from measurements and simulation using best fit $U_0 = 1.7 \times 10^{-15} \text{ eV cm}^2$. (d) Measured density dependence of the PL decay time and relative yield, corresponding to the exciton-exciton annihilation coefficient $R_A = 5 \times 10^{-3} \text{ cm}^2/\text{s}$.

values and varying R_A and U_0 parameters (see Supplemental Material [41]). The resulting changes of the mean-squared displacement $\Delta\sigma^2$, corresponding to the increase of the PL emission area over time [131], are presented in Fig. 3(a) together with the measured data at selected densities. Interestingly, setting either R_A or U_0 strictly to zero demonstrates that neither the effective diffusivity $D_{\text{eff}} \propto \partial\sigma^2/\partial t$ nor the $\Delta\sigma^2(t)$ traces unambiguously identify the origin of the nonlinear propagation.

To distinguish annihilation and repulsion, we consider relative increase of the spatially and time-dependent PL instead, presented in Fig. 3(b) as $\Delta I_{\text{PL}} = [I_{\text{PL}}(t) - I_{\text{PL}}(0)]/I_{\text{PL,max}}$ from simulations. In the case of repulsion, the increase of the PL counts on the flanks of the excitation spot stem from the drift of the excitons toward outer regions. For annihilation only, the increase of ΔI_{PL} stems exclusively from linear diffusion and is very small. Experimentally, changes in ΔI_{PL} can be detected by extracting either differential spatial profiles at different times or PL transients at different positions. For example, the delay time τ_{max} of the maximum PL intensity rises with the increasing distance from the excitation spot in case of repulsion, as illustrated in Fig. 3(b).

The results of this analysis are presented in Fig. 3(c), demonstrating a characteristic feature of repulsion and determining the interaction constant $U_0 = 1.7 \times 10^{-15} \text{ eV cm}^2$ (see Supplemental Material [41] for detailed discussion). This interaction constant accounts for about one half of the observed increase of the effective diffusivity with excitation density. It is accompanied by a decrease of

the PL lifetime and relative yield [Fig. 3(c)] that are characteristic features of an efficient annihilation process with $R_A = 5 \times 10^{-3} \text{ cm}^2/\text{s}$. Consequently, both annihilation and repulsion are found to contribute to the nonlinear propagation of IXs in roughly equal measures in the studied sample; the corresponding simulated result is shown in Figs. 2(c) and 3(a).

In general, regardless of the origin of the density-dependent process, one typically finds subdiffusive behavior of the mean-squared displacement [24,27,32,33,35,131]. It involves rapid initial diffusion that decreases toward smaller values at later times. Interestingly, it is not the case for the studied high-density conditions in the vicinity of the Mott transition. This is demonstrated by the normalized space- and time-resolved PL image in Fig. 4(a) and the extracted $\Delta\sigma^2$ values in Fig. 4(b) (upper panel). The data show a rapid initial expansion during the first 50 ps followed by a contraction over several hundreds of picoseconds. This corresponds to an effective diffusion coefficient starting from $35 \text{ cm}^2/\text{s}$ and then decreasing to a negative value of $-5 \text{ cm}^2/\text{s}$, see upper panel of Fig. 4(c). At later times, the contraction slows down and the effective diffusion coefficient increases again.

The effectively negative diffusivity of IXs is a consistent observation in the studied heterobilayer (see Supplemental Material [41]), albeit a highly unusual one. This implies a substantial change in the dynamics of the optically excited electron-hole pairs associated with the Mott transition. While a contraction of a quasiparticle cloud can be related to density-induced many-particle states such as droplet

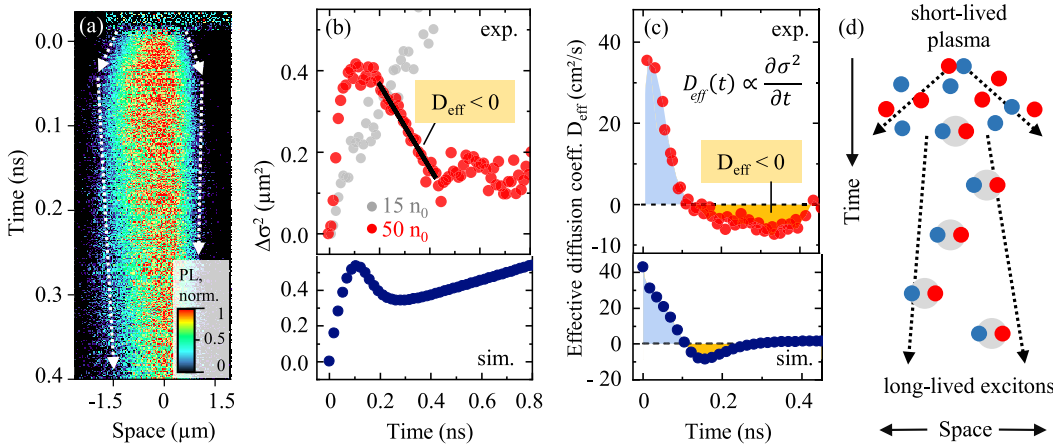


FIG. 4. (a) Streak camera image of the spatially and time-resolved PL at $T = 5$ K in the high-density regime of about $6 \times 10^{12} \text{ cm}^{-2}$ ($50n_0$, pump energy density: $25 \mu\text{J cm}^{-2}$) above the Mott transition; the PL intensity is normalized at each time step. (b) Upper: time-resolved mean-squared displacement in experiment comparing high ($50n_0$) and intermediate ($15n_0$) densities. (b) Lower: simulation results showing the implications of a generic two-component model: rapidly expanding, short-lived plasma and longer-lived, slower excitons. (c) Corresponding time-dependent effective diffusion coefficients extracted from $D_{\text{eff}} \propto \partial\sigma^2/\partial t$. (d) Schematic illustration of the two-component model.

formation (see Supplemental Material [41]), interplay of multiple types of propagating, transient excitations is often a more likely cause [132–134]. At the studied density conditions close to the Mott threshold, a possible scenario would involve rapid propagation of short-lived plasma, followed by a slower diffusion of a small fraction of long-lived excitons. As schematically shown in Fig. 4(d), this would effectively lead to a substantial broadening of the electron-hole distribution and a subsequent shrinking after the plasma recombines.

To illustrate the consequence of such a scenario, we use a simplified model with two components that both diffuse according to Eq. (1) (see Supplemental Material [41]). The resulting, simulated $\Delta\sigma^2$ and extracted, time-dependent diffusivity are presented in the lower panels of Figs. 4(b) and 4(c), respectively. This shows that a two-component diffusion involving plasma and excitons could indeed lead to the observed behavior. We note, however, that an appropriate microscopic description of these intriguing findings involving a dense many-particle system above the Mott threshold would be highly desirable.

In summary, we show that interlayer excitons in van der Waals heterostructures diffuse rapidly in the absence of moiré- and disorder-induced localization. Corresponding low-density diffusivity is about 1000 times higher compared to findings in moiré superlattices, with temperature dependence confirming free diffusion. At elevated excitation densities, we have demonstrated how the effects of exciton-exciton annihilation and repulsion can be distinguished with both providing substantial contributions to the nonlinear propagation. Density range of the Mott transition revealed an unusual behavior involving rapid initial expansion followed by a long-lived effectively negative diffusivity.

Altogether, these findings should allow for disentanglement of complexities associated with mobile dipolar excitons in van der Waals heterostructures across linear and nonlinear regimes, demonstrating a promising platform for exciton transport. The intriguing dynamics at the exciton-plasma crossover should be of particular interest for a broad community studying physics of interacting electron-hole quasiparticles and correlated many-body states.

We thank Sivan Refaelly-Abramson, Ronen Rapaport, Andreas Beer, Jonas Zipfel, and Archana Raja for helpful discussions, as well as Imke Gronwald, Christian Bäuml, and Nicola Paradiso for their assistance with prepatterned substrate preparation. Financial support by the DFG via SPP2244 (Project ID 443405595), Emmy Noether Initiative (CH 1672/1, Project ID: 287022282), SFB 1277 (Project-ID 314695032, project B05), the Würzburg-Dresden Cluster of Excellence on Complexity and Topology in Quantum Matter (ct.qmat) (EXC 2147, Project ID 390858490), and the Munich Center for Quantum Science and Technology (MCQST) (EXC 2111, Project ID 390814868) is gratefully acknowledged. A. H. acknowledges funding by the European Research Council (ERC) (Grant Agreement No. 772195). K. W. and T. T. acknowledge support from the JSPS KAKENHI (Grants No. 20H00354, No. 21H05233, and No. 23H02052) and World Premier International Research Center Initiative (WPI), MEXT, Japan. A. S. and M. F. would like to acknowledge resources for computational time at the HLRN (Göttingen/Berlin). M. F. acknowledges support by the Alexander von Humboldt Foundation.

- *alexey.chernikov@tu-dresden.de
- [1] A. K. Geim and I. V. Grigorieva, van der Waals heterostructures, *Nature (London)* **499**, 419 (2013).
- [2] K. S. Novoselov, A. Mishchenko, A. Carvalho, and A. H. Castro Neto, 2D materials and van der Waals heterostructures, *Science* **353** (2016).
- [3] C. Jin, E. Y. Ma, O. Karni, E. C. Regan, F. Wang, and T. F. Heinz, Ultrafast dynamics in van der Waals heterostructures, *Nat. Nanotechnol.* **13**, 994 (2018).
- [4] E. C. Regan, D. Wang, E. Y. Paik, Y. Zeng, L. Zhang, J. Zhu, A. H. MacDonald, H. Deng, and F. Wang, Emerging exciton physics in transition metal dichalcogenide heterobilayers, *Nat. Rev. Mater.* **7**, 778 (2022).
- [5] H. Yu, G.-B. Liu, J. Tang, X. Xu, and W. Yao, Moiré excitons: From programmable quantum emitter arrays to spin-orbit-coupled artificial lattices, *Sci. Adv.* **3**, e1701696 (2017).
- [6] F. Wu, T. Lovorn, and A. H. MacDonald, Topological exciton bands in Moiré heterojunctions, *Phys. Rev. Lett.* **118**, 147401 (2017).
- [7] N. Zhang, A. Surrente, M. Baranowski, D. K. Maude, P. Gant, A. Castellanos-Gomez, and P. Plochocka, Moiré intralayer excitons in a MoSe₂/MoS₂ heterostructure, *Nano Lett.* **18**, 7651 (2018).
- [8] C. Jin, E. C. Regan, A. Yan, M. Iqbal Bakti Utama, D. Wang, S. Zhao, Y. Qin, S. Yang, Z. Zheng, S. Shi, K. Watanabe, T. Taniguchi, S. Tongay, A. Zettl, and F. Wang, Observation of moiré excitons in WSe₂/WS₂ heterostructure superlattices, *Nature (London)* **567**, 76 (2019).
- [9] K. L. Seyler, P. Rivera, H. Yu, N. P. Wilson, E. L. Ray, D. G. Mandrus, J. Yan, W. Yao, and X. Xu, Signatures of moiré-trapped valley excitons in MoSe₂/WSe₂ heterobilayers, *Nature (London)* **567**, 66 (2019).
- [10] E. M. Alexeev *et al.*, Resonantly hybridized excitons in moiré superlattices in van der Waals heterostructures, *Nature (London)* **567**, 81 (2019).
- [11] K. Tran *et al.*, Evidence for moiré excitons in van der Waals heterostructures, *Nature (London)* **567**, 71 (2019).
- [12] Y. Xu, S. Liu, D. A. Rhodes, K. Watanabe, T. Taniguchi, J. Hone, V. Elser, K. F. Mak, and J. Shan, Correlated insulating states at fractional fillings of moiré superlattices, *Nature (London)* **587**, 214 (2020).
- [13] E. C. Regan, D. Wang, C. Jin, M. I. Bakti Utama, B. Gao, X. Wei, S. Zhao, W. Zhao, Z. Zhang, K. Yumigeta, M. Blei, J. D. Carlström, K. Watanabe, T. Taniguchi, S. Tongay, M. Crommie, A. Zettl, and F. Wang, Mott and generalized Wigner crystal states in WSe₂/WS₂ moiré superlattices, *Nature (London)* **579**, 359 (2020).
- [14] Y. Tang, L. Li, T. Li, Y. Xu, S. Liu, K. Barmak, K. Watanabe, T. Taniguchi, A. H. MacDonald, J. Shan, and K. F. Mak, Simulation of Hubbard model physics in WSe₂/WS₂ moiré superlattices, *Nature (London)* **579**, 353 (2020).
- [15] P. Merkl, F. Mooshammer, P. Steinleitner, A. Girnghuber, K.-Q. Lin, P. Nagler, J. Holler, C. Schüller, J. M. Lupton, T. Korn, S. Ovesen, S. Brem, E. Malic, and R. Huber, Ultrafast transition between exciton phases in van der Waals heterostructures, *Nat. Mater.* **18**, 691 (2019).
- [16] L. V. Butov, A. Zrenner, G. Abstreiter, G. Böhm, and G. Weimann, Condensation of indirect excitons in coupled AlAs/GaAs quantum wells, *Phys. Rev. Lett.* **73**, 304 (1994).
- [17] R. Rapaport, G. Chen, D. Snoke, S. H. Simon, L. Pfeiffer, K. West, Y. Liu, and S. Denev, Charge separation of dense two-dimensional electron-hole gases: Mechanism for exciton ring pattern formation, *Phys. Rev. Lett.* **92**, 117405 (2004).
- [18] P. Rivera, J. R. Schaibley, A. M. Jones, J. S. Ross, S. Wu, G. Aivazian, P. Klement, K. Seyler, G. Clark, N. J. Ghimire, J. Yan, D. G. Mandrus, W. Yao, and X. Xu, Observation of long-lived interlayer excitons in monolayer MoSe₂-WSe₂ heterostructures, *Nat. Commun.* **6**, 6242 (2015).
- [19] D. Unuchek, A. Ciarrocchi, A. Avsar, K. Watanabe, T. Taniguchi, and A. Kis, Room-temperature electrical control of exciton flux in a van der Waals heterostructure, *Nature (London)* **560**, 340 (2018).
- [20] P. Rivera, K. L. Seyler, H. Yu, J. R. Schaibley, J. Yan, D. G. Mandrus, W. Yao, and X. Xu, Valley-polarized exciton dynamics in a 2D semiconductor heterostructure, *Science* **351**, 688 (2016).
- [21] Z. Wang, D. A. Rhodes, K. Watanabe, T. Taniguchi, J. C. Hone, J. Shan, and K. F. Mak, Evidence of high-temperature exciton condensation in two-dimensional atomic double layers, *Nature* **574**, 76 (2019).
- [22] E. V. Calman, M. M. Fogler, L. V. Butov, S. Hu, A. Mishchenko, and A. K. Geim, Indirect excitons in van der Waals heterostructures at room temperature, *Nat. Commun.* **9**, 1895 (2018).
- [23] L. A. Jauregui, A. Y. Joe, K. Pistunova, D. S. Wild, A. A. High, Y. Zhou, G. Scuri, K. De Greve, A. Sushko, C.-H. Yu, T. Taniguchi, K. Watanabe, D. J. Needleman, M. D. Lukin, H. Park, and P. Kim, Electrical control of interlayer exciton dynamics in atomically thin heterostructures, *Science* **366**, 870 (2019).
- [24] L. Yuan, B. Zheng, J. Kunstmänn, T. Brumme, A. B. Kuc, C. Ma, S. Deng, D. Blach, A. Pan, and L. Huang, Twist-angle-dependent interlayer exciton diffusion in WS₂-WSe₂ heterobilayers, *Nat. Mater.* **19**, 617 (2020).
- [25] J. Choi, W.-T. Hsu, L.-S. Lu, L. Sun, H.-Y. Cheng, M.-H. Lee, J. Quan, K. Tran, C.-Y. Wang, M. Staab, K. Jones, T. Taniguchi, K. Watanabe, M.-W. Chu, S. Gwo, S. Kim, C.-K. Shih, X. Li, and W.-H. Chang, Moiré potential impedes interlayer exciton diffusion in van der Waals heterostructures, *Sci. Adv.* **6** (2020).
- [26] Z. Li, X. Lu, D. F. Cordovilla Leon, Z. Lyu, H. Xie, J. Hou, Y. Lu, X. Guo, A. Kaczmarek, T. Taniguchi, K. Watanabe, L. Zhao, L. Yang, and P. B. Deotare, Interlayer exciton transport in MoSe₂/WSe₂ heterostructures, *ACS Nano* **15**, 1539 (2021).
- [27] J. Wang, Q. Shi, E. M. Shih, L. Zhou, W. Wu, Y. Bai, D. Rhodes, K. Barmak, J. Hone, C. R. Dean, and X. Y. Zhu, Diffusivity reveals three distinct phases of interlayer excitons in MoSe₂/WSe₂ heterobilayers, *Phys. Rev. Lett.* **126**, 106804 (2021).
- [28] Z. Sun, A. Ciarrocchi, F. Tagarelli, J. F. Gonzalez Marin, K. Watanabe, T. Taniguchi, and A. Kis, Excitonic transport driven by repulsive dipolar interaction in a van der Waals heterostructure, *Nat. Photonics* **16**, 79 (2022).
- [29] A. Raja, L. Waldecker, J. Zipfel, Y. Cho, S. Brem, J. D. Ziegler, M. Kulig, T. Taniguchi, K. Watanabe, E. Malic,

- T. F. Heinz, T. C. Berkelbach, and A. Chernikov, Dielectric disorder in two-dimensional materials, *Nat. Nanotechnol.* **14**, 832 (2019).
- [30] Z. Vörös, R. Balili, D. W. Sone, L. Pfeiffer, and K. West, Long-distance diffusion of excitons in double quantum well structures, *Phys. Rev. Lett.* **94**, 226401 (2005).
- [31] M. Stern, V. Garmider, E. Segre, M. Rappaport, V. Umansky, Y. Levinson, and I. Bar-Joseph, Photoluminescence ring formation in coupled quantum wells: Excitonic versus ambipolar diffusion, *Phys. Rev. Lett.* **101**, 257402 (2008).
- [32] M. Kulig, J. Zipfel, P. Nagler, S. Blanter, C. Schüller, T. Korn, N. Paradiso, M. M. Glazov, and A. Chernikov, Exciton diffusion and halo effects in monolayer semiconductors, *Phys. Rev. Lett.* **120**, 207401 (2018).
- [33] A. J. Goodman, D.-H. Lien, G. H. Ahn, L. L. Spiegel, M. Amani, A. P. Willard, A. Javey, and W. A. Tisdale, Substrate-dependent exciton diffusion and annihilation in chemically treated MoS₂ and WS₂, *J. Phys. Chem. C* **124**, 12175 (2020).
- [34] J. Wang *et al.*, Optical generation of high carrier densities in 2D semiconductor heterobilayers, *Science Adv.* **5**, aax0145 (2019).
- [35] J. Choi, J. Embley, D. D. Blach, R. Perea-Causín, D. Erkensten, D. S. Kim, L. Yuan, W. Y. Yoon, T. Taniguchi, K. Watanabe, K. Ueno, E. Tutuc, S. Brem, E. Malic, X. Li, and L. Huang, Fermi pressure and Coulomb repulsion driven rapid hot plasma expansion in a van der Waals heterostructure, *Nano Lett.* **23**, 4399 (2023).
- [36] A. Weston *et al.*, Atomic reconstruction in twisted bilayers of transition metal dichalcogenides, *Nat. Nanotechnol.* **15**, 592 (2020).
- [37] M. R. Rosenberger, H.-J. Chuang, M. Phillips, V. P. Oleshko, K. M. McCreary, S. V. Sivaram, C. S. Hellberg, and B. T. Jonker, Twist angle-dependent atomic reconstruction and Moiré patterns in transition metal dichalcogenide heterostructures, *ACS Nano* **14**, 4550 (2020).
- [38] S. Zhao, Z. Li, X. Huang, A. Rupp, J. Göser, I. A. Vovk, S. Y. Kruchinin, K. Watanabe, T. Taniguchi, I. Bilgin, A. S. Baimuratov, and A. Högele, Excitons in mesoscopically reconstructed moiré heterostructures, *Nat. Nanotechnol.* **18**, 572 (2023).
- [39] M. Först, L. Colombier, R. K. Patel, J. Lindlau, A. D. Mohite, H. Yamaguchi, M. M. Glazov, D. Hunger, and A. Högele, Cavity-control of interlayer excitons in van der Waals heterostructures, *Nat. Commun.* **10**, 3697 (2019).
- [40] A. Castellanos-Gomez, M. Buscema, R. Molenaar, V. Singh, L. Janssen, H. S. J. van der Zant, and G. A. Steele, Deterministic transfer of two-dimensional materials by all-dry viscoelastic stamping, *2D Mater.* **1**, 011002 (2014).
- [41] See Supplemental Material at <http://link.aps.org/supplemental/10.1103/PhysRevLett.132.016202>, which includes Refs. [11,32,41–121], for additional experimental data, theoretical analysis, and discussion.
- [42] A. Jain, P. Bharadwaj, S. Heeg, M. Parzefall, T. Taniguchi, K. Watanabe, and L. Novotny, Minimizing residues and strain in 2D materials transferred from PDMS, *Nanotechnology* **29**, 265203 (2018).
- [43] Q. Tong, H. Yu, Q. Zhu, Y. Wang, X. Xu, and W. Yao, Topological mosaics in moiré superlattices of van der Waals heterobilayers, *Nat. Phys.* **13**, 356 (2017).
- [44] M. H. Naik, I. Maity, P. K. Maiti, and M. Jain, Kolmogorov-Crespi potential for multilayer transition-metal dichalcogenides: Capturing structural transformations in moiré superlattices, *J. Phys. Chem. C* **123**, 9770 (2019).
- [45] M. Phillips and C. S. Hellberg, Commensurate structures in twisted transition metal dichalcogenide heterobilayers, *arXiv:1909.02495*.
- [46] X. Zhao, Z. Ding, J. Chen, J. Dan, S. M. Poh, W. Fu, S. J. Pennycook, W. Zhou, and K. P. Loh, Strain modulation by van der Waals coupling in bilayer transition metal dichalcogenide, *ACS Nano* **12**, 1940 (2018).
- [47] X. Hu, L. Kou, and L. Sun, Stacking orders induced direct band gap in bilayer MoSe₂-WSe₂ lateral heterostructures, *Sci. Rep.* **6**, 31122 (2016).
- [48] R. Suzuki, M. Sakano, Y. J. Zhang, R. Akashi, D. Morikawa, A. Harasawa, K. Yaji, K. Kuroda, K. Miyamoto, T. Okuda, K. Ishizaka, A. R., and Y. Iwasa, Valley-dependent spin polarization in bulk MoS₂ with broken inversion symmetry, *Nat. Nanotechnol.* **9**, 611 (2014).
- [49] W.-T. Hsu, Z.-A. Zhao, L.-J. Li, C.-H. Chen, M.-H. Chiu, P.-S. Chang, Y.-C. Chou, and W.-H. Chang, Second harmonic generation from artificially stacked transition metal dichalcogenide twisted bilayers, *ACS Nano* **8**, 2951 (2014).
- [50] I. Paradisano, Andres Manuel Saiz Raven, T. Amand, C. Robert, P. Renucci, K. Watanabe, T. Taniguchi, I. C. Gerber, X. Marie, and B. Urbaszek, Second harmonic generation control in twisted bilayers of transition metal dichalcogenides, *Phys. Rev. B* **105**, 115420 (2022).
- [51] Y. Li, Y. Rao, K. Mak, Y. You, S. Wang, C. Dean, and T. F. Heinz, Probing symmetry properties of few-layer MoS₂ and h-BN by optical second-harmonic generation, *Nano Lett.* **13**, 3329 (2013).
- [52] W. Kim, J. Y. Ahn, J. Oh, J. H. Shim, and S. Ryu, Second-harmonic Young's interference in atom-thin heterocrystals, *Nano Lett.* **20**, 8825 (2020).
- [53] A. M. van der Zande, J. Kunstmänn, A. Chernikov, D. A. Chenet, Y. You, X. Zhang, P. Y. Huang, T. C. Berkelbach, L. Wang, F. Zhang, M. S. Hybertsen, D. A. Muller, D. R. Reichman, T. F. Heinz, and J. C. Hone, Tailoring the electronic structure in bilayer molybdenum disulfide via interlayer twist, *Nano Lett.* **14**, 3869 (2014).
- [54] J. Zipfel, K. Wagner, M. A. Semina, J. D. Ziegler, T. Taniguchi, K. Watanabe, M. M. Glazov, and A. Chernikov, Electron recoil effect in electrically tunable MoSe₂ monolayers, *Phys. Rev. B* **105**, 075311 (2022).
- [55] A. Singh, G. Moody, S. Wu, Y. Wu, N. J. Ghimire, J. Yan, D. G. Mandrus, X. Xu, and X. Li, Coherent electronic coupling in atomically thin MoSe₂, *Phys. Rev. Lett.* **112**, 216804 (2014).
- [56] J. S. Ross, S. Wu, H. Yu, N. J. Ghimire, A. M. Jones, G. Aivazian, J. Yan, D. G. Mandrus, D. Xiao, W. Yao, and X. Xu, Electrical control of neutral and charged excitons in a monolayer semiconductor, *Nat. Commun.* **4**, 1474 (2013).

- [57] A. M. Jones, H. Yu, N. J. Ghimire, S. Wu, G. Aivazian, J. S. Ross, B. Zhao, J. Yan, D. G. Mandrus, D. Xiao, W. Yao, and X. Xu, Optical generation of excitonic valley coherence in monolayer WSe₂, *Nat. Nanotechnol.* **8**, 634 (2013).
- [58] E. Liu, J. van Baren, Z. Lu, M. M. Altaiary, T. Taniguchi, K. Watanabe, D. Smirnov, and C. H. Lui, Gate tunable dark trions in monolayer WSe₂, *Phys. Rev. Lett.* **123**, 027401 (2019).
- [59] X.-X. Zhang, Y. You, Shu Yang Frank Zhao, and T. F. Heinz, Experimental evidence for dark excitons in monolayer WSe₂, *Phys. Rev. Lett.* **115**, 257403 (2015).
- [60] M. He, P. Rivera, D. Van Tuan, N. P. Wilson, M. Yang, T. Taniguchi, K. Watanabe, J. Yan, D. G. Mandrus, H. Yu, H. Dery, W. Yao, and X. Xu, Valley phonons and exciton complexes in a monolayer semiconductor, *Nat. Commun.* **11**, 618 (2020).
- [61] K. F. Mak, K. He, C. Lee, G. H. Lee, J. Hone, T. F. Heinz, and J. Shan, Tightly bound trions in monolayer MoS₂, *Nat. Mater.* **12**, 207 (2013).
- [62] A. Esser, R. Zimmermann, and E. Runge, Theory of trion spectra in semiconductor nanostructures, *Phys. Status Solidi (b)* **227**, 317 (2001).
- [63] D. K. Efimkin, E. K. Laird, J. Levinsen, M. M. Parish, and A. H. MacDonald, Electron-exciton interactions in the exciton-polaron problem, *Phys. Rev. B* **103**, 075417 (2021).
- [64] A. Kormányos, G. Burkard, M. Gmitra, J. Fabian, V. Zólyomi, N. D. Drummond, and V. Fal'ko, $\mathbf{p} \cdot \mathbf{k}$ theory for two-dimensional transition metal dichalcogenide semiconductors, *2D Mater.* **2**, 022001 (2015).
- [65] C. Robert, D. Lagarde, F. Cadiz, G. Wang, B. Lassagne, T. Amand, A. Balocchi, P. Renucci, S. Tongay, B. Urbaszek, and X. Marie, Exciton radiative lifetime in transition metal dichalcogenide monolayers, *Phys. Rev. B* **93**, 205423 (2016).
- [66] H. H. Fang, B. Han, C. Robert, M. A. Semina, D. Lagarde, E. Courtade, T. Taniguchi, K. Watanabe, T. Amand, B. Urbaszek, M. M. Glazov, and X. Marie, Control of the exciton radiative lifetime in van der Waals heterostructures, *Phys. Rev. Lett.* **123**, 067401 (2019).
- [67] N. Kumar, Q. Cui, F. Ceballos, D. He, Y. Wang, and H. Zhao, Exciton-exciton annihilation in MoSe₂ monolayers, *Phys. Rev. B* **89**, 125427 (2014).
- [68] S. Mouri, Y. Miyauchi, M. Toh, W. Zhao, G. Eda, and K. Matsuda, Nonlinear photoluminescence in atomically thin layered WSe₂ arising from diffusion-assisted exciton-exciton annihilation, *Phys. Rev. B* **90**, 155449 (2014).
- [69] L. Yuan, T. Wang, T. Zhu, M. Zhou, and L. Huang, Exciton dynamics, transport, and annihilation in atomically thin two-dimensional semiconductors, *J. Phys. Chem. Lett.* **8**, 3371 (2017).
- [70] D. Sun, Y. Rao, G. A. Reider, G. Chen, Y. You, L. Brézin, A. R. Harutyunyan, and T. F. Heinz, Observation of rapid exciton-exciton annihilation in monolayer molybdenum disulfide, *Nano Lett.* **14**, 5625 (2014).
- [71] Y. Hoshi, T. Kuroda, M. Okada, R. Moriya, S. Masubuchi, K. Watanabe, T. Taniguchi, R. Kitaura, and T. Machida, Suppression of exciton-exciton annihilation in tungsten disulfide monolayers encapsulated by hexagonal boron nitrides, *Phys. Rev. B* **95**, 241403(R) (2017).
- [72] A. F. Rigosi, H. M. Hill, Y. Li, A. Chernikov, and T. F. Heinz, Probing interlayer interactions in transition metal dichalcogenide heterostructures by optical spectroscopy: MoS₂/WS₂ and MoSe₂/WSe₂, *Nano Lett.* **15**, 5033 (2015).
- [73] H. Li, S. Li, M. H. Naik, J. Xie, X. Li, J. Wang, E. Regan, D. Wang, W. Zhao, S. Zhao, S. Kahn, K. Yumigeta, M. Blei, T. Taniguchi, K. Watanabe, S. Tongay, A. Zettl, S. G. Louie, F. Wang, and M. F. Crommie, Imaging moiré flat bands in three-dimensional reconstructed WSe₂/WS₂ superlattices, *Nat. Mater.* **20**, 945 (2021).
- [74] S. Carr, D. Massatt, S. B. Torrisi, P. Cazeaux, M. Luskin, and E. Kaxiras, Relaxation and domain formation in incommensurate two-dimensional heterostructures, *Phys. Rev. B* **98**, 224102 (2018).
- [75] V. V. Enaldiev, F. Ferreira, S. J. Magorrian, and V. I. Fal'ko, Piezoelectric networks and ferroelectric domains in twistronic superlattices in WS₂/MoS₂ and WSe₂/MoSe₂ bilayers, *2D Mater.* **8**, 025030 (2021).
- [76] A. Rodríguez, J. Varillas, G. Haider, M. Kalbáč, and F. Otakar, Complex strain scapes in reconstructed transition-metal dichalcogenide moiré superlattices, *ACS Nano* **17**, 7787 (2023).
- [77] F. Dirnberger, J. D. Ziegler, P. E. F. Junior, R. Bushati, T. Taniguchi, K. Watanabe, J. Fabian, D. Bougeard, A. Chernikov, and V. M. Menon, Quasi-1D exciton channels in strain-engineered 2D materials, *Sci. Adv.* **7**, eabj3066 (2021).
- [78] E. M. Alexeev, A. Catanzaro, O. V. Skrypka, P. K. Nayak, S. Ahn, S. Pak, J. Lee, J. I. Sohn, K. S. Novoselov, H. S. Shin, and A. I. Tartakovskii, Imaging of interlayer coupling in van der Waals heterostructures using a bright-field optical microscope, *Nano Lett.* **17**, 5342 (2017).
- [79] D. H. Luong, H. S. Lee, G. P. Neupane, S. Roy, G. Ghimire, J. H. Lee, Q. A. Vu, and Y. H. Lee, Tunneling photocurrent assisted by interlayer excitons in staggered van der Waals hetero-bilayers, *Adv. Mater.* **29**, 1701512 (2017).
- [80] K. Wagner, Z. A. Iakovlev, J. D. Ziegler, M. Cuccu, T. Taniguchi, K. Watanabe, M. M. Glazov, and A. Chernikov, Diffusion of excitons in a two-dimensional Fermi sea of free charges, *Nano Lett.* **23**, 4708 (2023).
- [81] M. Selig, G. Berghäuser, A. Raja, P. Nagler, C. Schüller, T. F. Heinz, T. Korn, A. Chernikov, E. Malic, and A. Knorr, Excitonic linewidth and coherence lifetime in monolayer transition metal dichalcogenides, *Nat. Commun.* **7**, 13279 (2016).
- [82] M. M. Glazov, Z. A. Iakovlev, and S. Refaelly-Abramson, Phonon-induced exciton weak localization in two-dimensional semiconductors, *Appl. Phys. Lett.* **121**, 192106 (2022).
- [83] R. Perea-Causín, S. Brem, R. Rosati, R. Jago, M. Kulig, J. D. Ziegler, J. Zipfel, A. Chernikov, and E. Malic, Exciton propagation and halo formation in two-dimensional materials, *Nano Lett.* **19**, 7317 (2019).
- [84] M. M. Glazov, Phonon wind and drag of excitons in monolayer semiconductors, *Phys. Rev. B* **100**, 045426 (2019).
- [85] D. Erkensten, S. Brem, R. Perea-Causín, and E. Malic, Microscopic origin of anomalous interlayer exciton

- transport in van der Waals heterostructures, *Phys. Rev. Mater.* **6**, 094006 (2022).
- [86] W. Kohn, Cyclotron resonance and de Haas–Van Alphen oscillations of an interacting electron gas, *Phys. Rev.* **123**, 1242 (1961).
- [87] B. Laikhtman and R. Rapaport, Exciton correlations in coupled quantum wells and their luminescence blue shift, *Phys. Rev. B* **80**, 195313 (2009).
- [88] C. Schindler and R. Zimmermann, Analysis of the exciton-exciton interaction in semiconductor quantum wells, *Phys. Rev. B* **78**, 045313 (2008).
- [89] L. H. Fowler-Gerace, Z. Zhou, E. A. Szwed, and L. V. Butov, Long-range quantum transport of indirect excitons in van der Waals heterostructure, [arxiv.2204.09760](https://arxiv.org/abs/2204.09760).
- [90] D. W. deQuilettes, R. Brenes, M. Laitz, B. T. Motes, M. M. Glazov, and V. Bulović, Impact of photon recycling, grain boundaries, and nonlinear recombination on energy transport in semiconductors, *ACS Photonics* **9**, 110 (2022).
- [91] Y. E. Lozovik and V. I. Yudson, Feasibility of superfluidity of paired spatially separated electrons and holes; a new superconductivity mechanism, *Sov. J. Exp. Theor. Phys. Lett.* **22**, 274 (1975), http://jetpletters.ru/ps/1530/article_23399.pdf.
- [92] M. M. Glazov and R. A. Suris, Collective states of excitons in semiconductors, *Phys. Usp.* **63**, 1051 (2021).
- [93] L. D. Landau and E. M. Lifshitz, *Fluid Mechanics* (Pergamon Press, New York, 1987), [10.1016/c2013-0-03799-1](https://doi.org/10.1016/c2013-0-03799-1).
- [94] E. A. Kuznetsov and M. Y. Kagan, Semiclassical expansion of quantum gases into a vacuum, *Theor. Math. Phys.* **202**, 399 (2020).
- [95] A. A. Kurilovich, V. N. Mantsevich, Y. Mardoukh, K. J. Stevenson, A. V. Chechkin, and V. V. Palyulin, Non-Markovian diffusion of excitons in layered perovskites and transition metal dichalcogenides, *Phys. Chem. Chem. Phys.* **24**, 13941 (2022).
- [96] M. M. Fogler, L. V. Butov, and K. S. Novoselov, High-temperature superfluidity with indirect excitons in van der Waals heterostructures, *Nat. Commun.* **5**, 4555 (2014).
- [97] A. Kumar and P. Ahluwalia, Tunable dielectric response of transition metals dichalcogenides MX_2 ($M = Mo, W$; $X = S, Se, Te$): Effect of quantum confinement, *Physica (Amsterdam)* **407B**, 4627 (2012).
- [98] D. Erkensten, S. Brem, R. Perea-Causín, and E. Malic, Microscopic origin of anomalous interlayer exciton transport in van der Waals heterostructures, *Phys. Rev. Mater.* **6**, 094006 (2022).
- [99] D. Semkat, F. Richter, D. Kremp, G. Manzke, W.-D. Kraeft, and K. Henneberger, Ionization equilibrium in an excited semiconductor: Mott transition versus Bose-Einstein condensation, *Phys. Rev. B* **80**, 155201 (2009).
- [100] P. Giannozzi *et al.*, QUANTUM ESPRESSO: A modular and open-source software project for quantum simulations of materials, *J. Phys. Condens. Matter* **21**, 395502 (2009).
- [101] P. Giannozzi *et al.*, Advanced capabilities for materials modelling with QUANTUM ESPRESSO, *J. Phys. Condens. Matter* **29**, 465901 (2017).
- [102] J. P. Perdew, K. Burke, and M. Ernzerhof, Generalized gradient approximation made simple, *Phys. Rev. Lett.* **78**, 1396(E) (1997).
- [103] M. J. van Setten, M. Giantomassi, E. Bousquet, M. J. Verstraete, D. R. Hamann, X. Gonze, and G. M. Rignanese, The PseudoDojo: Training and grading a 85 element optimized norm-conserving pseudopotential table, *Comput. Phys. Commun.* **226**, 39 (2018).
- [104] R. Gillen and J. Maultzsch, Interlayer excitons in $MoSe_2/WSe_2$ heterostructures from first principles, *Phys. Rev. B* **97**, 165306 (2018).
- [105] S. Grimme, J. Antony, S. Ehrlich, and H. Krieg, A consistent and accurate *ab initio* parametrization of density functional dispersion correction (DFT-D) for the 94 elements H-Pu, *J. Chem. Phys.* **132**, 154104 (2010).
- [106] K. Nakamura, Y. Yoshimoto, Y. Nomura, T. Tadano, M. Kawamura, T. Kosugi, K. Yoshimi, T. Misawa, and Y. Motoyama, RESPACK: An *ab initio* tool for derivation of effective low-energy model of material, *Comput. Phys. Commun.* **261**, 107781 (2021).
- [107] A. Steinhoff, F. Jahnke, and M. Florian, Microscopic theory of exciton-exciton annihilation in two-dimensional semiconductors, *Phys. Rev. B* **104**, 155416 (2021).
- [108] G. Schönhoff, M. Rösner, R. E. Groenewald, S. Haas, and T. O. Wehling, Interplay of screening and superconductivity in low-dimensional materials, *Phys. Rev. B* **94**, 134504 (2016).
- [109] C. Steinke, T. O. Wehling, and M. Rösner, Coulomb-engineered heterojunctions and dynamical screening in transition metal dichalcogenide monolayers, *Phys. Rev. B* **102**, 115111 (2020).
- [110] M. Rösner, E. Şaşioğlu, C. Friedrich, S. Blügel, and T. O. Wehling, Wannier function approach to realistic Coulomb interactions in layered materials and heterostructures, *Phys. Rev. B* **92**, 085102 (2015).
- [111] R. Resta, Thomas-Fermi dielectric screening in semiconductors, *Phys. Rev. B* **16**, 2717 (1977).
- [112] M. Florian, M. Hartmann, A. Steinhoff, J. Klein, A. W. Holleitner, J. J. Finley, T. O. Wehling, M. Kaniber, and C. Gies, The dielectric impact of layer distances on exciton and trion binding energies in van der Waals heterostructures, *Nano Lett.* **18**, 2725 (2018).
- [113] Z. Gong, G.-B. Liu, H. Yu, D. Xiao, X. Cui, X. Xu, and W. Yao, Magnetoelectric effects and valley-controlled spin quantum gates in transition metal dichalcogenide bilayers, *Nat. Commun.* **4**, 2053 (2013).
- [114] D. Kremp, M. Schlanges, and W.-D. Kraeft, *Quantum Statistics of Nonideal Plasmas* (Springer, Berlin, 2005).
- [115] D. Erben, A. Steinhoff, C. Gies, G. Schönhoff, T. O. Wehling, and F. Jahnke, Excitation-induced transition to indirect band gaps in atomically thin transition-metal dichalcogenide semiconductors, *Phys. Rev. B* **98**, 035434 (2018).
- [116] A. Schobert, J. Berges, E. G. C. P. van Loon, M. A. Sentef, S. Brener, M. Rossi, and T. O. Wehling, *Ab initio* electron-lattice downfolding: Potential energy landscapes, anharmonicity, and molecular dynamics in charge density wave materials, [arXiv:2303.07261](https://arxiv.org/abs/2303.07261).
- [117] A. Segura, L. Artús, R. Cuscó, T. Taniguchi, G. Cassabois, and B. Gil, Natural optical anisotropy of *h*-BN highest giant birefringence in a bulk crystal through the mid-infrared to ultraviolet range, *Phys. Rev. Mater.* **2**, 024001 (2018).

- [118] V. G. Karpov, Negative diffusion and clustering of growing particles, *Phys. Rev. Lett.* **75**, 2702 (1995).
- [119] P. Argyrakis, A. A. Chumak, M. Maragakis, and N. Tsakiris, Negative diffusion coefficient in a two-dimensional lattice-gas system with attractive nearest-neighbor interactions, *Phys. Rev. B* **80**, 104203 (2009).
- [120] A. L. Efros, Negative density of states: Screening, Einstein relation, and negative diffusion, *Phys. Rev. B* **78**, 155130 (2008).
- [121] K. Wagner, E. Wietek, J. D. Ziegler, M. A. Semina, T. Taniguchi, K. Watanabe, J. Zipfel, M. M. Glazov, and A. Chernikov, Autoionization and dressing of excited excitons by free carriers in monolayer WSe₂, *Phys. Rev. Lett.* **125**, 267401 (2020).
- [122] E. Barré, O. Karni, E. Liu, A. L. O’Beirne, X. Chen, H. B. Ribeiro, L. Yu, B. Kim, K. Watanabe, T. Taniguchi, K. Barmak, C. H. Lui, S. Refaelly-Abramson, F. H. da Jornada, and T. F. Heinz, Optical absorption of interlayer excitons in transition-metal dichalcogenide heterostructures, *Science* **376**, 406 (2022).
- [123] M. Brotons-Gisbert, H. Baek, A. Campbell, K. Watanabe, T. Taniguchi, and B. D. Gerardot, Moiré-trapped interlayer triplons in a charge-tunable WSe₂/MoSe₂ heterobilayer, *Phys. Rev. X* **11**, 031033 (2021).
- [124] E. Liu, E. Barré, J. van Baren, M. Wilson, T. Taniguchi, K. Watanabe, Y.-T. Cui, N. M. Gabor, T. F. Heinz, Y.-C. Chang, and C. H. Lui, Signatures of moiré triplons in WSe₂/MoSe₂ heterobilayers, *Nature (London)* **594**, 46 (2021).
- [125] X. Wang, J. Zhu, K. L. Seyler, P. Rivera, H. Zheng, Y. Wang, M. He, T. Taniguchi, K. Watanabe, J. Yan, D. G. Mandrus, D. R. Gamelin, W. Yao, and X. Xu, Moiré triplons in MoSe₂/WSe₂ heterobilayers, *Nat. Nanotechnol.* **16**, 1208 (2021).
- [126] P. E. Faria Junior and J. Fabian, Signatures of electric field and layer separation effects on the spin-valley physics of MoSe₂/WSe₂ heterobilayers: From energy bands to dipolar excitons, *Nanomater. Nanotechnol.* **13**, 1187 (2023).
- [127] K. Wagner, J. Zipfel, R. Rosati, E. Wietek, J. D. Ziegler, S. Brem, R. Perea-Causín, T. Taniguchi, K. Watanabe, M. M. Glazov, E. Malic, and A. Chernikov, Nonclassical exciton diffusion in monolayer WSe₂, *Phys. Rev. Lett.* **127**, 076801 (2021).
- [128] J. Zipfel, M. Kulig, R. Perea-Causín, S. Brem, J. D. Ziegler, R. Rosati, T. Taniguchi, K. Watanabe, M. M. Glazov, E. Malic, and A. Chernikov, Exciton diffusion in monolayer semiconductors with suppressed disorder, *Phys. Rev. B* **101**, 115430 (2020).
- [129] A. Steinhoff, M. Florian, M. Rösner, G. Schönhoff, T. O. Wehling, and F. Jahnke, Exciton fission in monolayer transition metal dichalcogenide semiconductors, *Nat. Commun.* **8**, 1166 (2017).
- [130] R. Rapaport, G. Chen, and S. H. Simon, Nonlinear dynamics of a dense two-dimensional dipolar exciton gas, *Phys. Rev. B* **73**, 033319 (2006).
- [131] N. S. Ginsberg and W. A. Tisdale, Spatially resolved photogenerated exciton and charge transport in emerging semiconductors, *Annu. Rev. Phys. Chem.* **71**, 1 (2020).
- [132] R. Rosati, K. Wagner, S. Brem, R. Perea-Causín, E. Wietek, J. Zipfel, J. D. Ziegler, M. Selig, T. Taniguchi, K. Watanabe, A. Knorr, A. Chernikov, and E. Malic, Temporal evolution of low-temperature phonon sidebands in transition metal dichalcogenides, *ACS Photonics* **7**, 2756 (2020).
- [133] J. D. Ziegler, J. Zipfel, B. Meisinger, M. Menahem, X. Zhu, T. Taniguchi, K. Watanabe, O. Yaffe, D. A. Egger, and A. Chernikov, Fast and anomalous exciton diffusion in two-dimensional hybrid perovskites, *Nano Lett.* **20**, 6674 (2020).
- [134] D. Beret, L. Ren, C. Robert, L. Foussat, P. Renucci, D. Lagarde, A. Balocchi, T. Amand, B. Urbaszek, K. Watanabe, T. Taniguchi, X. Marie, and L. Lombez, Non-linear diffusion of negatively charged excitons in monolayer WSe₂, *Phys. Rev. B* **107**, 045420 (2023).